Journal of Alloys and Compounds 787 (2019) 1097–1103

Contents lists available at ScienceDirect

Journal of Alloys and Compounds

journal homepage: http://www.elsevier.com/locate/jalcom

Thin and broadband $Ce_2Fe_{17}N_{3-\delta}$/MWCNTs composite absorber with efficient microwave absorption

An Ling [a, b, c], Jing Pan [a, *], Guoguo Tan [b, c, **], Xisheng Gu [b, c], Yaxin Lou [b, c], Shuwen Chen [b, c], Qikui Man [b, c], Run-Wei Li [b, c], Xincai Liu [a]

[a] School of Material Science and Chemical Engineering, Ningbo University, Ningbo 315211, China
[b] Key Laboratory of Magnetic Materials and Devices, Ningbo Institute of Materials Technology & Engineering, Chinese Academy of Sciences, Ningbo, Zhejiang, 315201, China
[c] Zhejiang Province Key Laboratory of Magnetic Materials and Application Technology, Ningbo Institute of Materials Technology & Engineering, Chinese Academy of Sciences, Ningbo, Zhejiang, 315201, China

ARTICLE INFO

Article history:
Received 7 November 2018
Received in revised form
11 February 2019
Accepted 13 February 2019
Available online 14 February 2019

Keywords:
Microwave absorption
Multi-walled carbon nanotubes
Reflection loss
Effective absorption bandwidth
Impedance matching

ABSTRACT

Microwave absorption composites consisting of $Ce_2Fe_{17}N_{3-\delta}$ and various weight ratios of multi-walled carbon nanotubes (MWCNTs) (0, 0.5, 1, 1.5 wt%) as absorbers were prepared, and their microwave absorption performance was investigated. The results show that the composites attain increasing complex permittivity as the loading ratio of MWCNTs increase, whereas the permeability is almost unaffected. The composite filled with 0.5 wt% of the MWCNTs had a minimum reflection loss (RL) of −48.7 dB and effective absorption bandwidth (EAB, with an RL of less than −10 dB) of 5.5 GHz at a thickness of 1.4 mm. Owing to the balance of the ameliorated impedance conditions and the synergetic effect of dielectric and magnetic loss, the microwave absorption performance was enhanced significantly.

1. Introduction

With the rapidly increasing application of electromagnetic waves (EMWs), a superior-performance absorber is urgently needed for the purpose of eliminating adverse EMWs, not only for military stealth, but also for electronic-device compatibility and the reduction of EMWs pollution [1–4]. 3C (computer, communication, and consumer electronics) products [5] are also needed microwave absorbing materials to eliminate harmful EMWs. To obtain high absorbing performance, such as a wide absorption frequency range and strong absorption properties [6], the impedance of the materials should be well-matched and they should possess excellent absorbing capabilities. A proper impedance ratio between the materials and air ensures that EMWs can enter the interior rather than be reflected from the interface [7]. The absorption bandwidth can be broadened efficiently if proper impedance ratios are obtained in a wide frequency range. Therefore, obtaining a good impedance matching ratio is a necessary precondition for achieving excellent absorbing performance. In addition, the attenuation capability of the material ensures that incident EMWs can be attenuated inside the material.

In general, complex permittivity ($\varepsilon_r = \varepsilon' - j\varepsilon''$) and permeability ($\mu_r = \mu' - j\mu''$) are two major parameters of microwave absorbing materials (MAMs) that influence the input impedance and attenuation capability [8–10]. Using a composite is a simple approach to achieve the unique physical properties required [11–13]. Filling materials that can easily alter electric or magnetic properties have become a common solution to obtain excellent absorption. It is well known that the complex permittivity and permeability of a filler absorber are determined by the property and volume fraction of the filler, internal structure of the composites, and microwave frequency [14]. Niu et al. [15] fabricated a 3D conductive network composed of Co-Ni-P/SiC through an easy electroless plating method to improve the dielectric loss, obtaining a minimum RL of −45 dB at 12.5 GHz with a thickness of only 1.5 mm. The excellent microwave absorption was attributed to dielectric and magnetic loss as well as improved impedance matching. Therefore, a

* Correponding author.
** Corresponding author. Key Laboratory of Magnetic Materials and Devices, Ningbo Institute of Materials Technology & Engineering, Chinese Academy of Sciences, Ningbo, Zhejiang, 315201, China.
E-mail addresses: panjing@nbu.edu.cn (J. Pan), kant01@126.com (G. Tan).

https://doi.org/10.1016/j.jallcom.2019.02.164
0925-8388/

balance between impedance and attenuation can be likely achieved by using a proper ratio of the composite.

Recently, carbon materials such as carbon nanotubes (CNTs) [16,17], graphite [18], graphene [19,20], porous carbon [21] have been widely utilized in MAMs for high dielectric loss and physical properties. Sun [22] investigated aligned CNT films at a thickness of 2 mm and achieved a minimum RL value of −19 dB, but with a narrow bandwidth of 2.1 GHz, where MWCNTs exhibit a boost in the electrical loss ability. Singh [23] prepared hierarchical CNTs grown on carbon fiber that exhibited an RL of −42 dB and EAB of 2.7 GHz at 2.5 mm. However, because of the high permittivity, an absorber with good impedance is difficult to implement with only carbon materials, and excellent absorbing performance is hard to achieve. As they are limited to a single electrical loss absorbing mechanism, carbon materials often show narrow bandwidth. The studies mentioned herein have improved an aspect of the absorbing performance, but the bandwidth is not sufficient for application. In previous work by other researchers, magnetic particles filled with CNTs, such as carbonyl iron [24,25], ferroferric oxide [26–28], and ceramics [29–31] have been widely investigated. The experimental results show that the absorption performances of these MAMs were enhanced with the synergistic effect between magnetic particles and CNTs. Ge [32] blended the CNTs and CI@SiO_2 with paraffin, obtaining a minimum RL of −51.54 dB and EAB of 6.08 GHz. Chen et al. [33] reported an advanced HWCNTs/Fe@Fe_3O_4 absorber which exhibited a large EAB of 5.4 GHz with a thickness of 1.5 mm and a minimum RL of −41 dB at 1.9 mm. Wang et al. [34] prepared an absorber composed of $NiCo_2$/10%CNTs which achieved 4.4 GHz for EAB and −25.5 dB for minimum RL. This composite showed various electromagnetic loss forms. It has become a hot spot to combine the CNTs with magnetic loss materials to achieve a superior absorption performance. High complex permeability materials, such as rare-earth materials, as single filler have been applied in EMW absorbing field. Qiao [35] fabricated a $Ce_{1.8}Sm_{0.2}Fe_{17}N_{3-\delta}$/paraffin composite and achieved a minimum RL of −39 dB. Gu [36] investigated the microwave absorption performance of $Ce_2Fe_{17}N_{3-\delta}$ powders/silicone composites whose RL is less than −10 dB in the whole X-band. However, although carbon materials and high-magnetic-loss materials can achieve high absorption values, their own bandwidth is not ideal. Therefore, combining CNTs with high permittivity and $Ce_2Fe_{17}N_{3-\delta}$ to generate a synergism of electric and magnetic loss may be an effective and simple way to achieve high absorbing performance.

Herein, an absorber of $Ce_2Fe_{17}N_{3-\delta}$/MWCNTs paraffin composites is presented to fulfil the requirements of thin thickness, broadband characteristic and strong absorption. The complex permittivity and permeability, as well as RL, were analyzed in detailed at the frequency region of 2–18 GHz. In this study, the influences of different contents of MWCNTs loading and RL were explored at fixed thicknesses. The balance between microwave absorption performance and impedance matching is the primary determinant in the improvement of microwave absorption. Additionally, the loading of MWCNTs can also lead to more reflection and scattering of microwaves to increase the length of propagation path, resulting in more electromagnetic attenuation.

2. Experimental details

The Ce_2Fe_{17} ingots were prepared with high-purity cerium and iron via induction-melting in an Ar atmosphere protection, then Ce_2Fe_{17} ribbons were fabricated by melt-spinning and smashed to chips, followed by ball milling with absolute ethanol to obtain particles of uniform size. The $Ce_2Fe_{17}N_{3-\delta}$ powders were fabricated by nitrogenation of the ball-milled particles reacting with high-purity nitrogen gas for 1 h at 743 K in a stainless tube. The MWCNTs, provided by Beijing Dk Nano technology Co., LTD (Beijing, China), had an outer diameter of 8–15 nm and a length of 50 μm. The MWCNTs had a purity of 98% and had a bulk density of approximately 0.27 g/cm^3.

To investigate the characteristics and properties of composites made from different weight contents of MWCNTs loading, samples containing $Ce_2Fe_{17}N_{3-\delta}$ particles and various MWCNTs were fabricated and tested. In this experiment, the matrixes with 15 vol% $Ce_2Fe_{17}N_{3-\delta}$ and 85 vol% paraffin were mixed uniformly, (hexane was used as a solvent). Then 0, 0.5, 1, and 1.5 wt% MWCNTs of $Ce_2Fe_{17}N_{3-\delta}$ and paraffin were added to the composites. To obtain stable absorption performance, the composites were dispersed completely by stirring using an ultrasonic bath. The composites were placed in a fume hood for 6 h to ensure that the hexane evaporated completely; then, paraffin samples were fabricated with an outer diameter of 7.0 mm and inner diameter of 3.04 mm by pressing the composites in a mold (under a pressure of 2×10^4 kg).

The crystal phases were investigated by X-ray diffraction (XRD, Bruker AXS, Cu -Kα radiation). The morphology and structure of the particles were analyzed by scanning electron microscopy (SEM, FEI Quanta FEG 250 and Hitachi S-4800). The MWCNTs were studied using Transmission electron microscopy (TEM, JEOL-2100 microscope). The complex permittivity and permeability of the composites were determined to be in the 2–18 GHz range using an Agilent N5234A vector network analyzer.

3. Results and discussion

In Fig. 1(a), the XRD pattern of $Ce_2Fe_{17}N_{3-\delta}$ shows that the particles had a rhombohedral Th_2Zn_{17}-type structure [37]; and a few instances of α-Fe were noticed, which appeared during the nitrogenation process. After the nitrogenation process, nitrogen atoms entered Ce_2Fe_{17} as an interstitial atom [36]. The SEM image of $Ce_2Fe_{17}N_{3-\delta}$ particles is presented in Fig. 1(b). The $Ce_2Fe_{17}N_{3-\delta}$ particles were irregular thin flakes less than 1 μm in thickness and 2–5 μm in diameter. Fig. 1(c) shows the TEM image of the MWCNTs. The untreated MWCNTs showed a tendency for entanglement and agglomeration due to the intermolecular van der Waals force

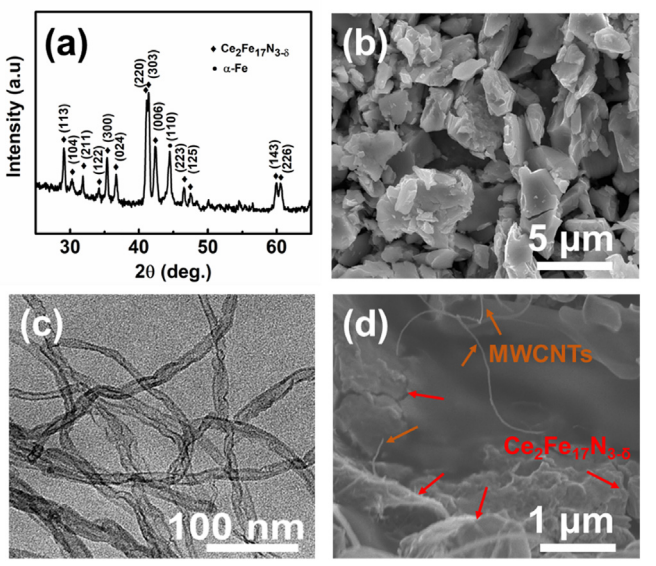

Fig. 1. (a) XRD pattern of $Ce_2Fe_{17}N_{3-\delta}$ particles, (b) SEM image of $Ce_2Fe_{17}N_{3-\delta}$ particles, (c) TEM image of MWCNTs, and (d) SEM image of $Ce_2Fe_{17}N_{3-\delta}$/MWCNTs composite with the 0.5 wt% MWCNTs loading.

between the MWCNTs even if the sample was exposed to ultrasound in ethanol. Fig. 1(d) presents the dispersion status of the $Ce_2Fe_{17}N_{3-\delta}$ and MWCNTs. From the SEM image of the slice of the composite, MWCNTs were uniformly dispersed in the matrix, and $Ce_2Fe_{17}N_{3-\delta}$ particles were wrapped absolutely by the paraffin. The MWCNTs, which were difficult to form in clusters, may result from the paraffin as barrier during ultrasonic agitation. Furthermore, a 3D internal conductive network was constructed owing to the pairing of MWCNTs and $Ce_2Fe_{17}N_{3-\delta}$ particles.

The complex permittivity and permeability of the samples at 2–18 GHz with the MWCNTs contents increasing from 0 to 1.5 wt%, including the real part and the imaginary part, are shown in Fig. 2. As shown in Fig. 2(a), the value of the real part of permittivity at 2 GHz reached 8.7, 12.4, 16.1, and 22.2, when the MWCNTs loadings were 0, 0.5, 1.0, and 1.5 wt% respectively. The values of the imaginary part of permittivity were 0.5, 2.0, 3.9, and 6.6 at 2 GHz, as seen in Fig. 2(b). The real part of permittivity showed a dramatic frequency dependence and decreased with increasing frequency. The value of the real part of permittivity decreased from 22.2 to 13.1 with 1.5 wt% MWCNTs loading in the measured frequency region. The imaginary part of the permittivity remained kept nearly constant throughout the frequency range. In addition, the values of complex permittivity of composites increased significantly with the increase of MWCNTs loading because of the high permittivity of MWCNTs. The polarization relaxation caused by MWCNTs may enhance the permittivity in the microwave range. Fig. 2(c) and (d) are the real part and the imaginary part of the permeability of matrices, respectively. In general, the microwave magnetic loss of magnetic materials originates mainly from hysteresis, domain wall resonance, eddy current loss, and natural ferromagnetic resonance [38]. The magnetic loss mainly depends on the property and loading ratios of magnetic particles ($Ce_2Fe_{17}N_{3-\delta}$), because MWCNTs are non-magnetic materials. With the same $Ce_2Fe_{17}N_{3-\delta}$ loading ratio, the permittivity shows an analogous tendency and value. The real parts of permeability at the starting frequency are in the range of 2.55–2.88 and 1.03–1.19 at the stop frequency. The values of the imaginary part of the permeability were between 0.3 and 0.5 over the entire testing frequency range, and showed a small fluctuation.

The attenuation constant (α) of samples which can express the dissipation capability of the absorber, was calculated in the measured frequency range using the following equation [39–41]:

$$\alpha = \frac{\sqrt{2}\pi f}{c} \times \sqrt{(\mu''\varepsilon'' - \mu'\varepsilon') + \sqrt{(\mu''\varepsilon'' - \mu'\varepsilon')^2 + (\mu''\varepsilon' + \mu'\varepsilon'')^2}} \quad (1)$$

where c and f are the velocity of light and the frequency, respectively. The curves of the calculated results are displayed in Fig. 3. It is clear that the attenuation constant of the samples increased with frequency, indicating superior absorption properties in the higher-frequency region. In addition, the matrix shows a larger α value as the weight fraction of the MWCNTs increase, which may be due to the higher dielectric loss.

Fig. 4 shows the typical frequency dependence on RL with various loading contents of MWCNTs at fixed thicknesses of 1.0, 1.4, 1.6, and 2.0 mm in the 2–18 GHz range. The EMWs reflection loss can be calculated by the following equations [42,43] according to the transmission line theory:

$$Z_{in} = Z_0\sqrt{\frac{\mu_r}{\varepsilon_r}}\tanh j\frac{2\pi ft}{c}\sqrt{\mu_r\varepsilon_r} \quad (2)$$

$$\mathrm{RL} = -20\lg\left|\frac{Z_{in} - Z_0}{Z_{in} + Z_0}\right| \quad (3)$$

where Z_{in} is input impedance of the sample, Z_0 is the impedance of air, ε_r and μ_r are the relative complex permittivity and relative complex permeability, respectively, f is the frequency, t is the thickness of the sample and c is the velocity of light.

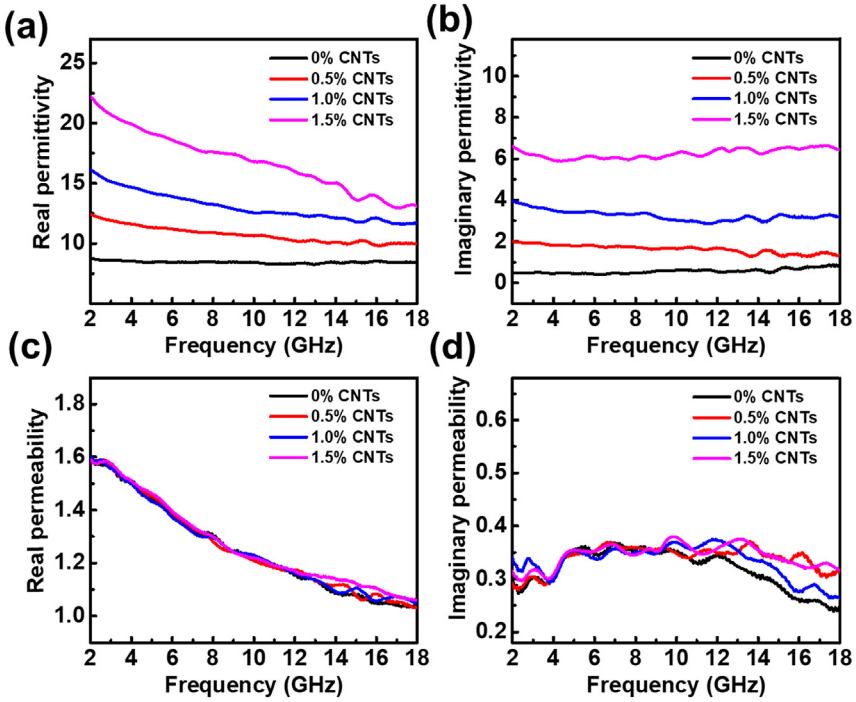

Fig. 2. Frequency dependence of complex (a, b) permittivity and (c, d) permeability for the $Ce_2Fe_{17}N_{3-\delta}$/MWCNTs paraffin composites with the loading of 0, 0.5, 1, and 1.5 wt% MWCNTs.

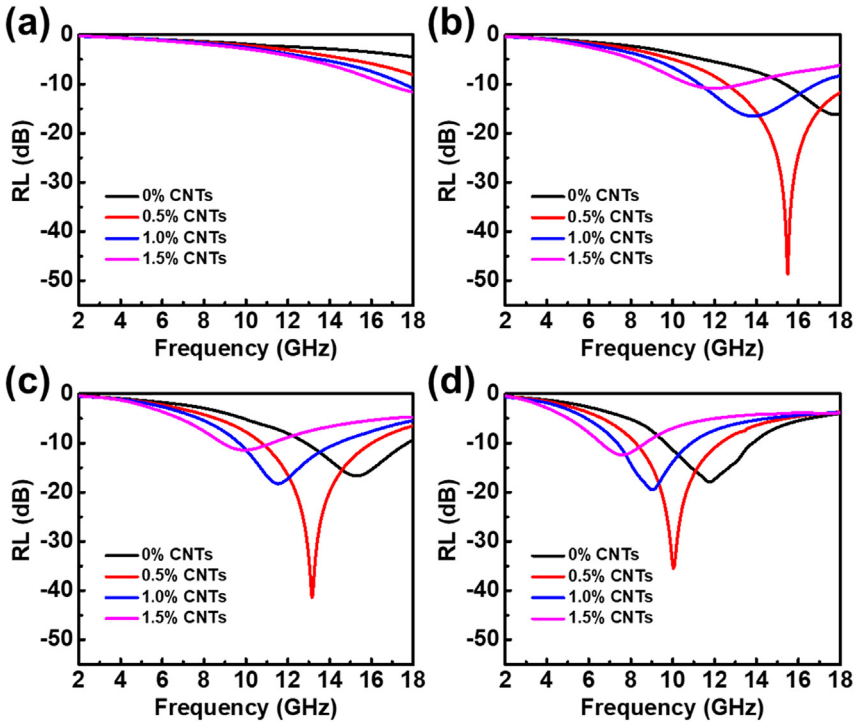

Fig. 3. Attenuation constant of $Ce_2Fe_{17}N_{3-\delta}$/MWCNTs composites.

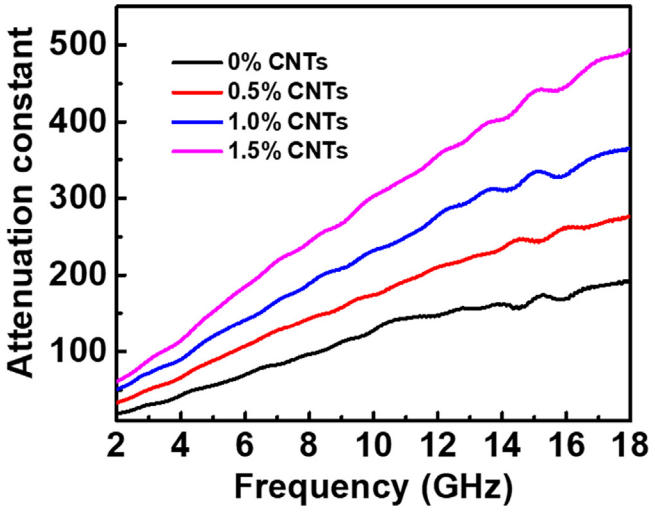

Fig. 4. RL curves for composites with 0, 0.5, 1, and 1.5 wt% MWCNTs loading, at thicknesses of (a) 1.0, (b) 1.4, (c) 1.6, and (d) 2.0 mm.

As shown in Fig. 4(a), 1.0-mm absorbers show a weak absorption in the measured frequency range. The minimum RL of −11.7 dB and EAB of 1.3 GHz were obtained with 1.5 wt% MWCNTs loading. The microwave absorption was significantly enhanced when the thickness came to 1.4 mm, as displayed in Fig. 4(b). The RL minimum value, obtained with 0.5 wt% MWCNTs loading at 1.4 mm, was −48.7 dB at 15.7 GHz. The absorber exhibited a superior performance with an EAB of 5.43 GHz. As observed in Fig. 4(c) and (d), the absorption peaks shift to the lower-frequency region. The absorbers with 0.5 wt% MWCNTs loading exhibited outstanding absorption compared with other MWCNTs loading values at the same thickness. Based on these results, the absorption performance is closely related to the loading content of MWCNTs and thickness of the absorber.

The minimum RL values of absorbers are statistics at various thicknesses between 1 and 2 mm, and the curves are displayed in Fig. 5(a). When the thickness was up to 1.2 mm or even larger, absorber could achieve −20 dB (99% reflection loss) and more-intense absorption, while MWCNTs loading gets to 0.5 wt%. At a loading ratio of 1 wt%, the absorption peak values were slightly increased at a lower thickness (1.0–1.4 mm). The small RL values indicate weakened absorption while the filling amount further

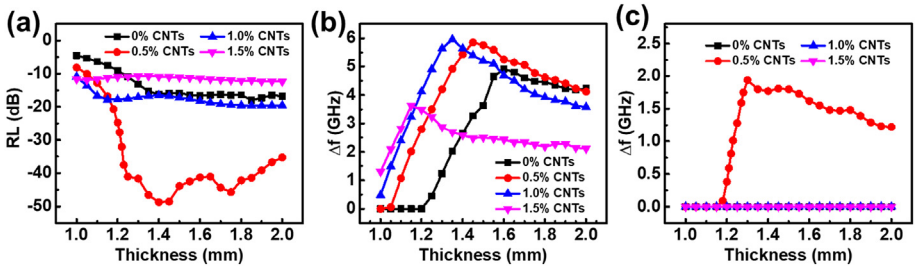

Fig. 5. Thickness dependence on (a) minimum RL, (b) EAB, and (c) absorption bandwidth when RL is less than −20 dB.

increased. This may be due primarily to the imbalance in the matching. Fig. 5(b) shows that the EAB of the absorbers broadened significantly in the thickness range of 1.0–1.5 mm and exhibited approximate bandwidth values with thicknesses beyond 1.5 mm at 0.5 wt% or 1.0 wt% loading. The calculated results show that the EAB attains approximately 6 GHz at 1.35 mm (1.0 wt% loading) and 1.45 mm (0.5 wt% loading). To some extent, a bandwidth of less than −20 dB is a particularly important feature to reflect the strong absorption performance of an absorber, as seen in Fig. 5(c). Only with a filling of 0.5 wt% MWCNTs can absorbers obtain the −20 dB absorption bandwidth.

The EMWs absorption performances were determined by the impedance matching condition [44] and attenuation characteristics of the materials. For good absorption, it is necessary that the impedance matching satisfies $Z_{in}/Z_0 = 1$. Therefore, the values of relative input dependence with each perfect matching condition were calculated, and the curve is shown in Fig. 6. For a 0% CNTs matrix, the values of Z_{in}/Z_0 are far from 1, showing a poor impedance matching condition. In other words, the EMWs are reflected drastically from the surface of the absorber, while a small number of EMWs entered it and were attenuated. For the 0.5 wt% MWCNTs loading, the values of Z_{in}/Z_0 are close to 1 in the higher-frequency region, indicating that the absorbers obtain good impedance matching conditions to ensure superior absorption performances. Combined with the attenuation constant, the proper content of MWCNTs loading can improve the absorption performances of the absorbers. Theoretically, the microwave attenuation should be as large as possible for strong absorption. However, although the attenuation increased as the MWCNTs loading ratios, the unbalanced impedance matching brought about a reduction in the absorption.

To investigate the EMWs absorbing mechanism of the absorber, Fig. 7(a) depicts the RL curves of $Ce_2Fe_{17}N_{3-\delta}$/MWCNTs paraffin composites with 0.5 wt% MWCNTs loading at 2–18 GHz. The frequencies corresponding to the minimum RL values shifted to the lower frequency region. As displayed in Fig. 7(b), the frequency dependence on thickness was calculated by a one-quarter wavelength model [45,46].

$$t_m = \frac{c}{4f_m\sqrt{|\mu_r||\varepsilon_r|}} \quad (4)$$

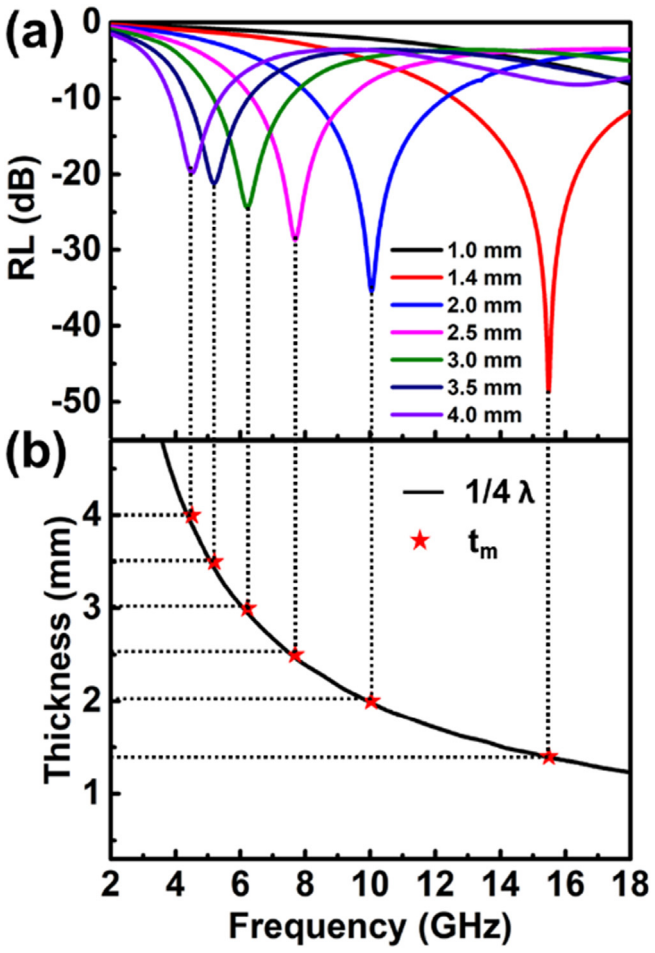

Fig. 7. (a) RL curves with seven thicknesses and (b) dependence of λ/4 absorber thickness on frequency of the $Ce_2Fe_{17}N_{3-\delta}$/MWCNTs paraffin composites with 0.5 wt% MWCNTs loading.

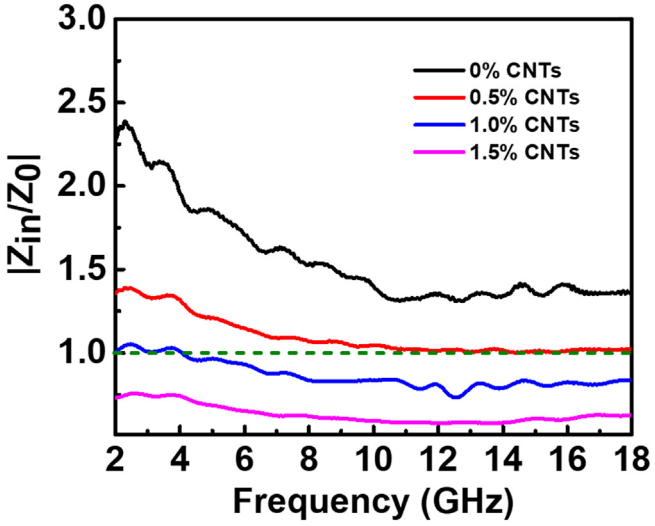

Fig. 6. Frequency dependence of relative input impedance for the various MWCNTs loading ratios.

where t_m and f_m are the matching thickness and absorption peak frequency, respectively. The red stars are the matching thicknesses of absorbers, and the frequencies are adapted with the absorption

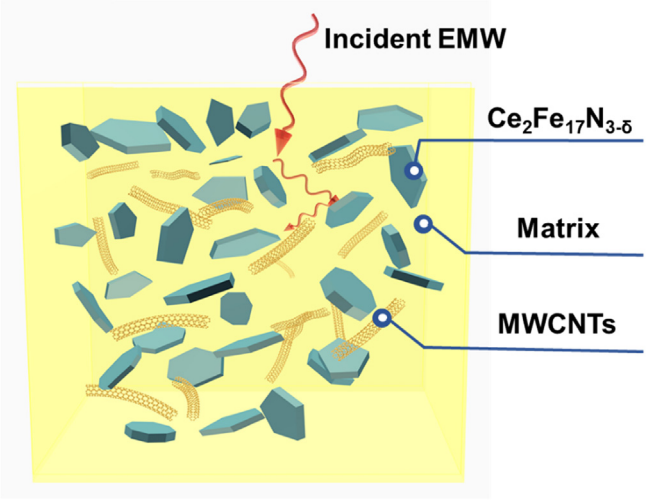

Fig. 8. (a) Attenuation mechanism in paraffin matrix and (b) multiple EMWs reflection in MWCNTs.

Table 1
Comparison of microwave absorption performance achieved by typical MWCNTs composites reported in recent literature and this work.

Composites	Magnetic-particle filling ratio	RL peak (dB)	EAB (GHz)	t_m (mm)	Ref
Al_2O_3/MWCNTs	40 vol%	−18.5	5.6(12.4–18)	1.84	[14]
Fe_2O_3/Fe_3O_4/MWCNTs	29 wt% Fe_2O_3/Fe_3O_4	−44.58	3.3(9.4–12.7)	2.4	[26]
ZnO/Fe_3O_4/MWCNTs	16.7 wt% Fe_3O_4	−38.2	2.1(5.1–7.2)	3.5	[27]
MWCNTs/$ZnFe_2O_4$	50 wt%	−55.5	3.6(12.2–15.8)	1.5	[29]
SnO_2/Fe_3O_4/MWCNTs	12.9 wt% Fe_3O_4	−42	2.8(9.6–12.4)	1.9	[47]
Zn ferrite/MWCNTs	60 wt%	−42.6	2.6(11–13.6)	1.5	[48]
NiFe alloy/MWCNTs	15 wt%	−19	2(8.2–10.2)	4	[49]
TiO_2/MWCNTs	30 wt%	−36.4	1.4(11–12.4)	2	[50]-1
Fe_2O_3/TiO_2/MWCNTs	15 wt%	−42.5	2.9(9.5–12.4)	2	[50]-2
$Ce_2Fe_{17}N_{3-\delta}$/MWCNTs	15 vol%	−48.7	5.5(12.5–18)	1.4	This work

peaks in Fig. 7(a). The six red stars denoting matching thicknesses and frequencies are located on the one-quarter wavelength matching curve, indicating that the relationship between peak frequency and thickness abides by the one-quarter wavelength model.

In general, the existence of MWCNTs provided numerous 3D conductive networks in the matrix, as shown in Fig. 8(a), resulting in more microwave attenuation. Additionally, multiple scatterings and polarization can be introduced in the matrix with the loading of MWCNTs, which can further increase the attenuation of microwaves, as displayed in Fig. 8(b). Above all, the superior microwave absorption performance was achieved by virtue of the balance of impedance matching and electromagnetic attenuation. The addition of MWCNTs improves the impedance matching with air and introduces higher electrical losses in the composite, greatly increasing the ability of EMWs to enter the absorber and undergo attenuation.

The microwave absorption performances achieved in previous work and in this study are listed in Table 1, and the performances with respect to the thicknesses and EAB, as well as RL, are shown in Fig. 9. Compared with other composites, $Ce_2Fe_{17}N_{3-\delta}$/MWCNTs exhibits excellent performance in minimum RL, bandwidth, and thickness, confirming that the composites in this study are potentially high-performance EMWs absorbing materials.

4. Conclusions

The $Ce_2Fe_{17}N_{3-\delta}$/MWCNTs paraffin composites were prepared with various contents of 0–1.5 wt% MWCNTs. For all specimens, the absorber with 0.5 wt% loading achieved superior performance because of the ideal balance in the impedance matching and electromagnetic attenuation. The minimum absorption was −48.7 dB at 15.7 GHz at a thickness of only 1.4 mm. Also, 5.5 GHz of EAB could be achieved with only 15 vol% magnetic-particle content filling. The excellent absorption performance results from the high electromagnetic loss and impedance matching for the proper ratio of permittivity and permeability at specific frequencies. The multiple scatterings and polarizations triggered by MWCNTs are also considered to have improved the microwave absorption.

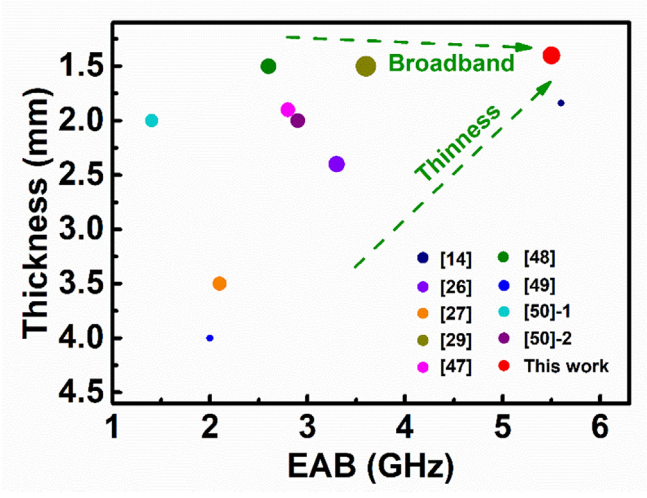

Fig. 9. Comparison in the thicknesses and EAB, as well as RL, of $Ce_2Fe_{17}N_{3-\delta}$/MWCNTs with other MWCNTs composite absorbers reported (the sizes of the circles represent the minimum RL).

Acknowledgments

This work was supported by the National Natural Science Foundation of China [grant number 51174121]; Ningbo National Natural Science Foundation [grant number 2018A610079]; Zhejiang Provincial Natural Science Foundation [grant number LQ19E010001].

References

[1] N. Li, G.W. Huang, Y.Q. Li, H.M. Xiao, Q.P. Feng, N. Hu, S.Y. Fu, Enhanced microwave absorption performance of coated carbon nanotubes by optimizing the Fe_3O_4 nanocoating structure, ACS Appl. Mater. Interfaces 9 (2017) 2973–2983.
[2] X. Su, J. Zhang, Y. Jia, Y. Liu, J. Xu, J. Wang, Preparation and microwave absorption property of nano onion-like carbon in the frequency range of 8.2-12.4 GHz, J. Alloys Compd. 695 (2017) 1420–1425.
[3] P. Wang, J. Zhang, Y. Chen, G. Wang, D. Wang, T. Wang, F. Li, Magnetism and microwave absorption properties of Fe_3O_4 microflake-paraffin composites without and with magnetic orientation, J. Electron. Mater. 47 (2018) 721–729.
[4] P. Liu, V.M.H. Ng, Z. Yao, J. Zhou, Y. Lei, Z. Yang, H. Lv, L.B. Kong, Facile synthesis and hierarchical assembly of flowerlike NiO structures with enhanced dielectric and microwave absorption properties, ACS Appl. Mater. Interfaces 9 (2017) 16404–16416.
[5] H. Pan, S. Zhang, J. Chen, M. Gao, Y. Liu, T. Zhu, Y. Jiang, Li- and Mn-rich layered oxide cathode materials for lithium-ion batteries: a review from fundamentals to research progress and applications, Mol. Syst. Des. Eng. 3 (2018) 748–803.
[6] Y. Liu, X. Su, F. Luo, J. Xu, J. Wang, X. He, Y. Qu, Facile synthesis and microwave absorption properties of double loss Ti_3SiC_2/Co_3Fe_7 powders, Ceram. Int. 44 (2018) 1995–2001.
[7] X. Li, X. Yin, C. Song, M. Han, H. Xu, W. Duan, L. Cheng, L. Zhang, Self-assembly core-shell graphene-bridged hollow MXenes spheres 3D foam with ultrahigh specific EM absorption performance, Adv. Funct. Mater. 28 (2018) 1803938.
[8] F. Wen, F. Zhang, Z. Liu, Investigation on microwave absorption properties for multiwalled carbon nanotubes/Fe/Co/Ni nanopowders as lightweight absorbers, J. Phys. Chem. C 115 (2011) 14025–14030.
[9] Y. Qing, W. Zhou, F. Luo, D. Zhu, Epoxy-silicone filled with multi-walled carbon nanotubes and carbonyl iron particles as a microwave absorber, Carbon 48 (2010) 4074–4080.
[10] R. Han, H. Yi, W. Zuo, T. Wang, L. Qiao, F. Li, Greatly enhanced permeability for planar anisotropy $Ce_2Fe_{17}N_{3-\delta}$ compound with rotational orientation in various external magnetic fields, J. Magn. Magn. Mater. 324 (2012) 2488–2491.
[11] X. Chen, Y. Huang, K. Zhang, W. Zhang, Cobalt fibers anchored with tin disulfide nanosheets as high-performance anode materials for lithium ion batteries, J. Colloid Interface Sci. 506 (2017) 291–299.
[12] X. Chen, Y. Huang, K. Zhang, Cobalt nanofibers coated with layered nickel silicate coaxial core-shell composites as excellent anode materials for lithium

ion batteries, J. Colloid Interface Sci. 513 (2018) 788–796.
[13] X. Chen, Y. Huang, X. Han, K. Zhang, Synthesis of cobalt nanofibers@nickel sulfide nanosheets hierarchical core-shell composites for anode materials of lithium ion batteries, Electrochim. Acta 284 (2018) 418–426.
[14] Y. Qing, X. Wang, Y. Zhou, Z. Huang, F. Luo, W. Zhou, Enhanced microwave absorption of multi-walled carbon nanotubes/epoxy composites incorporated with ceramic particles, Compos. Sci. Technol. 102 (2014) 161–168.
[15] F. Niu, Y. Wang, L. Ma, Z. Xie, Y. Wang, C. Wang, Y. Mao, Achieving enhanced dielectric property via growing Co-Ni-P nano-alloys on SiC nanowires with 3D conductive network, J. Alloys Compd. 778 (2019) 933–941.
[16] B. Zhao, X. Zhang, X. Fu, C. McCarthy, Synthesis of Fe3O4 hollow nanospheres-carbon nanotubes nanocomposites for the enhancement of dielectric heating performance, Mater. Lett. 235 (2019) 31–34.
[17] L. Yu, X. Lan, C. Wei, X. Li, X. Qi, T. Xu, MWCNT/NiO-Fe_3O_4 hybrid nanotubes for efficient electromagnetic wave absorption, J. Alloys Compd. 748 (2018) 111–116.
[18] C. Wang, R. Lv, Z. Huang, F. Kang, J. Gu, Synthesis and microwave absorbing properties of FeCo alloy particles/graphite nanoflake composites, J. Alloys Compd. 509 (2011) 494–498.
[19] P. Liu, V.M.H. Ng, Z. Yao, J. Zhou, Y. Lei, Z. Yang, L.B. Kong, Microwave absorption properties of double-layer absorbers based on $Co_{0.2}Ni_{0.4}Zn_{0.4}Fe_2O_4$ ferrite and reduced graphene oxide composites, J. Alloys Compd. 701 (2017) 841–849.
[20] P. Liu, Z. Yao, J. Zhou, Z. Yang, L. Bing Kong, Small magnetic Co-doped NiZn ferrite/graphene nanocomposites and their dual-region microwave absorption performance, J. Mater. Chem. C 4 (2016) 9738–9749.
[21] T. Huang, Z. Wu, Q. Yu, D. Tan, L. Li, Preparation of hierarchically porous carbon/magnetic particle composites with broad microwave absorption bandwidth, Chem. Eng. J. 359 (2019) 69–78.
[22] H. Sun, R. Che, X. You, Y. Jiang, Z. Yang, J. Deng, L. Qiu, H. Peng, Cross-stacking aligned carbon-nanotube films to tune microwave absorption frequencies and increase absorption intensities, Adv. Mater. 26 (2014) 8120–8125.
[23] S.K. Singh, M.J. Akhtar, K.K. Kar, Hierarchical carbon nanotube-coated carbon fiber: ultra lightweight, thin, and highly efficient microwave absorber, ACS Appl. Mater. Interfaces 10 (2018) 24816–24828.
[24] Y. Xu, L. Yuan, J. Cai, D. Zhang, Smart absorbing property of composites with MWCNTs and carbonyl iron as the filler, J. Magn. Magn. Mater. 343 (2013) 239–244.
[25] M. Jafarian, S.S.S. Afghahi, Y. Atassi, M. Salehi, Enhanced microwave absorption characteristics of nanocomposite based on hollow carbonyl iron microspheres and polyaniline decorated with MWCNTs, J. Magn. Magn. Mater. 462 (2018) 153–159.
[26] L. Huang, X. Liu, R. Yu, Enhanced microwave absorption properties of rod-shaped Fe_2O_3/Fe_3O_4/MWCNTs composites, Prog. Nat. Sci. 28 (2018) 288–295.
[27] L. Wang, H. Xing, Z. Liu, Z. Shen, X. Sun, G. Xu, Synthesis and excellent microwave absorption properties of ZnO/Fe_3O_4/MWCNTs composites, Nano 11 (2016) 1650139.
[28] Z. Liu, N. Zhao, C. Shi, F. He, E. Liu, C. He, Synthesis of three-dimensional carbon networks decorated with Fe3O4 nanoparticles as lightweight and broadband electromagnetic wave absorber, J. Alloys Compd. 776 (2019) 691–701.
[29] R. Shu, G. Zhang, X. Wang, X. Gao, M. Wang, Y. Gan, J. Shi, J. He, Fabrication of 3D net-like MWCNTs/$ZnFe_2O_4$ hybrid composites as high-performance electromagnetic wave absorbers, Chem. Eng. J. 337 (2018) 242–255.
[30] C. Ge, L. Wang, G. Liu, R. Wu, Effects of calcination temperature on the electromagnetic properties of carbon nanotubes/indium tin oxide composites, J. Alloys Compd. 775 (2019) 647–656.
[31] Y. Lan, X. Li, Y. Zong, Z. Li, Y. Sun, G. Tan, J. Feng, Z. Ren, X. Zheng, In-situ synthesis of carbon nanotubes decorated by magnetite nanoclusters and their applications as highly efficient and enhanced microwave absorber, Ceram. Int. 42 (2016) 19110–19118.
[32] C. Ge, L. Wang, G. Liu, T. Wang, Enhanced electromagnetic properties of carbon nanotubes and SiO_2-coated carbonyl iron microwave absorber, J. Alloys Compd. 767 (2018) 173–180.
[33] C. Chen, S. Bao, B. Zhang, Y. Chen, W. Chen, C. Wang, Coupling Fe@Fe3O4 nanoparticles with multiple-walled carbon nanotubes with width band electromagnetic absorption performance, Appl. Surf. Sci. 467–468 (2019) 836–843.
[34] B. Wang, C. Zhang, C. Mu, R. Yang, J. Xiang, J. Song, F. Wen, Z. Liu, Enhanced electromagnetic wave absorption properties of NiCo2 nanoparticles interspersed with carbon nanotubes, J. Magn. Magn. Mater. 471 (2019) 185–191.
[35] G. Qiao, W. Yang, Y. Lai, G. Tian, L. Zha, Q. Hu, S. Liu, C. Wang, J. Han, H. Du, Y. Yang, J. Yang, Crystal structure, magnetic and microwave absorption properties of $Ce_{2-x}Sm_xFe_{17}N_{3-\delta}$/paraffin composites, Mater. Res. Express 6 (2018), 016103.
[36] X. Gu, G. Tan, S. Chen, Q. Man, C. Chang, X. Wang, R.-W. Li, S. Che, L. Jiang, Microwave absorption properties of planar-anisotropy $Ce_2Fe_{17}N_{3-\delta}$ powders/Silicone composite in X-band, J. Magn. Magn. Mater. 424 (2017) 39–43.
[37] J.M.D. Coey, P.A.I. Smith, Magnetic nitrides, J. Magn. Magn. Mater. 200 (1999) 405–424.
[38] G. Tan, Y. Zhang, L. Qiao, T. Wang, J. Wang, F. Li, High-frequency electromagnetic properties of soft magnetic $Y_2Fe_{17}N_x$ particles with easy-plane anisotropy, Physica B 477 (2015) 52–55.
[39] Y. Liu, Z. Chen, Y. Zhang, R. Feng, X. Chen, C. Xiong, L. Dong, Broadband and lightweight microwave absorber constructed by in situ growth of hierarchical $CoFe_2O_4$/reduced graphene oxide porous nanocomposites, ACS Appl. Mater. Interfaces 10 (2018) 13860–13868.
[40] P. Liu, Z. Yao, V.M.H. Ng, J. Zhou, L.B. Kong, K. Yue, Facile synthesis of ultrasmall Fe_3O_4 nanoparticles on MXenes for high microwave absorption performance, Compos. Part A Appl. S. 115 (2018) 371–382.
[41] Y. Liu, Y. Li, F. Luo, X. Su, J. Xu, J. Wang, X. He, Y. Qu, Electromagnetic and microwave absorption properties of SiO_2-coated Ti_3SiC_2 powders with higher oxidation resistance, J. Alloys Compd. 715 (2017) 21–28.
[42] J.R. Liu, M. Itoh, K. Machida, Electromagnetic wave absorption properties of α-Fe/Fe_3B/Y_2O_3 nanocomposites in gigahertz range, Appl. Phys. Lett. 83 (2003) 4017–4019.
[43] P. Singh, V.K. Babbar, A. Razdan, R.K. Puri, T.C. Goel, Complex permittivity, permeability, and X-band microwave absorption of CaCoTi ferrite composites, J. Appl. Phys. 87 (2000) 4362–4366.
[44] X. Huang, J. Zhang, W. Rao, T. Sang, B. Song, C. Wong, Tunable electromagnetic properties and enhanced microwave absorption ability of flaky graphite/cobalt zinc ferrite composites, J. Alloys Compd. 662 (2016) 409–414.
[45] H. Wu, G. Wu, Y. Ren, L. Yang, L. Wang, X. Li, Co^{2+}/Co^{3+} ratio dependence of electromagnetic wave absorption in hierarchical $NiCo_2O_4$-$CoNiO_2$ hybrids, J. Mater. Chem. C 3 (2015) 7677–7690.
[46] J. Feng, F. Pu, Z. Li, X. Li, X. Hu, J. Bai, Interfacial interactions and synergistic effect of CoNi nanocrystals and nitrogen-doped graphene in a composite microwave absorber, Carbon 104 (2016) 214–225.
[47] L. Wang, H. Xing, Z. Liu, Z. Shen, X. Sun, G. Xu, Facile synthesis of net-like Fe_3O_4/MWCNTs decorated by SnO_2 nanoparticles as a highly efficient microwave absorber, RSC Adv. 6 (2016) 97142–97151.
[48] Z. Liu, H. Xing, Y. Liu, H. Wang, H. Jia, X. Ji, Hydrothermally synthesized Zn ferrite/multi-walled carbon nanotubes composite with enhanced electromagnetic-wave absorption performance, J. Alloys Compd. 731 (2018) 745–752.
[49] M.K. Naidu, K. Ramji, B.V.S.R.N. Santhosi, K.K. Murthy, C. Subrahmanyam, B. Satyanarayana, Influence of NiFe alloy nanopowder on electromagnetic and microwave absorption properties of MWCNT/epoxy composite, Adv. Polym. Technol. 37 (2018) 622–628.
[50] P. Bhattacharya, S. Sahoo, C.K. Das, Microwave absorption behaviour of MWCNT based nanocomposites in X-band region, Express Polym. Lett. 7 (2013) 212–223.